Virology **270,** 377–385 (2000)
doi:10.1006/viro.2000.0312, available online at http://www.idealibrary.com on IDEAL®

Molecular Studies on Bromovirus Capsid Protein

VI. Contributions of the N-Terminal Arginine-Rich Motif of BMV Capsid Protein to Virion Stability and RNA Packaging

Yoon Gi Choi, George L. Grantham, and A. L. N. Rao[1]

Department of Plant Pathology, University of California, Riverside, California 92521-0122

Received February 8, 2000; returned to author for revision February 29, 2000; accepted March 10, 2000

Specific interactions are likely to occur between the highly conserved N-proximal arginine-rich motif (ARM) of *Brome mosaic virus* (BMV) coat protein (CP) and each of three genomic RNAs and a single subgenomic RNA during *in vivo* encapsidation. To characterize these interactions, three independent deletions were engineered into a biologically active clone of BMV RNA3 (B3) such that the matured CP of each B3 variant precisely lacks either the entire ARM (B3/Δ919) or two consecutive arginine residues (B3/13ΔΔ14 and B3/18ΔΔ19) within the ARM. Analysis of virion RNA for each B3 variant recovered from symptomatic leaves of *Chenopodium quinoa* revealed that the interactions between the N-terminal ARM of BMV CP and each of three genomic RNAs is distinct. Northern blot hybridization of B3Δ919 virion RNA revealed that the deleted ARM region specifically affected the stability of virions containing RNA1. An abundant truncated RNA species recurrently found in the virions of B3Δ919 was identified to be a derivative of genomic RNA1, lacking the 5′ 943 nucleotides. Additional Northern blot analysis of virion RNAs from B3/Δ919, B3/13ΔΔ14, and B3/18ΔΔ19, and *in vitro* reassembly assays revealed that the N-terminal ARM region contains crucial amino acids required for RNA4 packaging, independent of genomic RNA3. The significance of these observations in relation to *Bromovirus* CP-RNA interactions during virion assembly is discussed.

INTRODUCTION

The coat proteins (CPs) of many plant viruses with icosahedral symmetry and containing single-stranded, (+) sense RNA genomes such as members of genera *Bromovirus*, *Cucumovirus*, *Sobemovirus,* and *Tombusvirus* have basic N-terminal arms that have been predicted to play an important role in RNA recognition during encapsidation *in vivo* (Fox *et al.,* 1994; Sacher and Ahlquist, 1989; Sgro *et al.,* 1986; Vriend *et al.,* 1986). In *Bromoviruses*, the basic environment is largely the result of the presence of a highly conserved N-terminal arginine-rich motif (hereafter referred to as ARM) (Fox *et al.,* 1994; Rao and Grantham, 1995; Sacher and Ahlquist, 1989). This arginine-rich domain, found in *Bromo* and *Cucumovirus* coat proteins (Rao and Grantham, 1996), bacterial antiterminators (Lazinski *et al.,* 1989), ribosomal proteins, and human immunodeficiency virus (HIV) Tat and Rev proteins (Burd and Dreyfuss, 1994; Tan and Frankel, 1995) recognizes specific regions in RNA when the peptide is in α-helical form. Vriend *et al.* (1986) suggested that the N-terminal arm of *Bromovirus* CP is flexible prior to interacting with viral RNA. This flexibility of the N-terminal arm is of great importance since it provides a mechanism to enhance the probability of interaction between protein and RNA. The large number of basic residues within the first 25 N-terminal amino acids in *Bromovirus* CPs [7 arginines and 1 lysine for *Brome mosaic virus* (BMV) and 6 arginines and 3 lysines in *Cowpea chlorotic mottle virus* (CCMV)] suggests that interaction between the negative phosphate groups in the RNA and the positive basic amino acids is important for nucleoprotein assembly. Based on *in vitro* analysis, it has been suggested that many nucleic acid binding proteins provide the best nucleic acid–protein interaction when the protein adapts an α-helical conformation (Van der Graaf *et al.,* 1992; Tan and Frankel, 1995).

The genome of BMV is divided among three genomic RNAs and the CP is synthesized from a single subgenomic RNA4 derived from progeny (−) RNA3 by internal initiation (Ahlquist, 1994). *Bromovirus* virions, with $T = 3$ symmetry, are assembled from 180 identical subunits of a single CP (Speir *et al.,* 1995). At present it is not known how a single BMV CP discriminates between each of the three genomic and a single subgenomic RNA and packages them into three individual particles of indistinguishable size and morphology. Previous deletion analysis of BMV CP N-terminal basic arm region demonstrated that variants lacking the N-proximal 7 but not 19 amino acids are biologically active and assembled into RNA containing virions *in vivo* (Rao and Grantham, 1995, 1996; Sacher and Ahlquist, 1989). These observations indicated that amino acid residues located be-

[1] To whom correspondence and reprint requests should be addressed. Fax: (603) 590-6673. E-mail: arao@ucrac1.ucr.edu

0042-6822/00 $35.00

tween 7 and 19 are intimately involved in interactions with each of the three genomic and the single subgenomic RNA. To precisely identify critical amino acid(s) of the ARM required for recognizing and packaging each BMV RNA, we have constructed and analyzed the biological activity and encapsidation competence of three BMV CP variants with defined deletions in the conserved ARM.

RESULTS AND DISCUSSION

Characteristics of B3/Δ919

The first 25 N-proximal amino acid region of *Bromovirus* CP is highly basic (Fig. 1A) and is not visible in the electron density map where it is thought to interact with the viral RNA inside the capsid shell (Speir *et al.,* 1995; Vriend *et al.,* 1986). A cluster of arginine residues providing the basic environment is located between amino acids 8 and 20 and is referred to as the N- terminal arginine-rich motif (ARM; Fig. 1A). To analyze the contribution of the ARM to BMV CP-RNA interactions during virion assembly, a sequence encoding 11 amino acids representing the ARM was precisely deleted from the CP gene in the cDNA clone of BMV RNA3 (B3). This deletion variant, referred to as B3/Δ919 (Fig. 1A), is expected to synthesize a CP devoid of five arginine residues contained within the designated ARM. When transcripts of B3/Δ919 are coinoculated with wild type (wt) BMV genomic RNAs 1 (B1) and 2 (B2) to barley protoplasts, the variant B3 replicated and synthesized subgenomic RNA4 but its accumulation levels are reduced by 90% as compared with that of wt (Fig. 1B). Since subgenomic RNA4 is derived from progeny (−) RNA3 (Miller *et al.,* 1985), interestingly no difference in the accumulation of progeny (−) RNA3 was observed when normalized against genomic RNAs 1 and 2 (Fig. 1B). However, truncated CPs translated from the subgenomic RNA4 of B3/Δ919 accumulated to wt levels (Fig. 1C). The reason for the reduced levels of subgenomic RNA4 of B3/Δ919 accumulation is not obvious, since several variants of B3 capable of synthesizing truncated CPs accumulated to near wt levels (Rao and Grantham, 1995, 1996). One possible explanation is that optimal recognition by viral replicase of the subgenomic RNA promoter on progeny (−) RNA3 requires the deleted sequence to maintain the spacial requirement. Alternatively, the stability of subgenomic RNA could have been affected by defective binding and or/packaging exhibited by the truncated CPs (see below).

In BMV infection, cell-to-cell movement and induction of visible local lesions in *C. quinoa* require both movement protein and CP (Schmitz and Rao,1996) and only those CP variants competent for virion assembly *in vivo* are able to induce local lesions (Rao and Grantham, 1995, 1996; Rao, 1999). Therefore, it could be tested directly whether truncated CP of B3/Δ919 is capable of

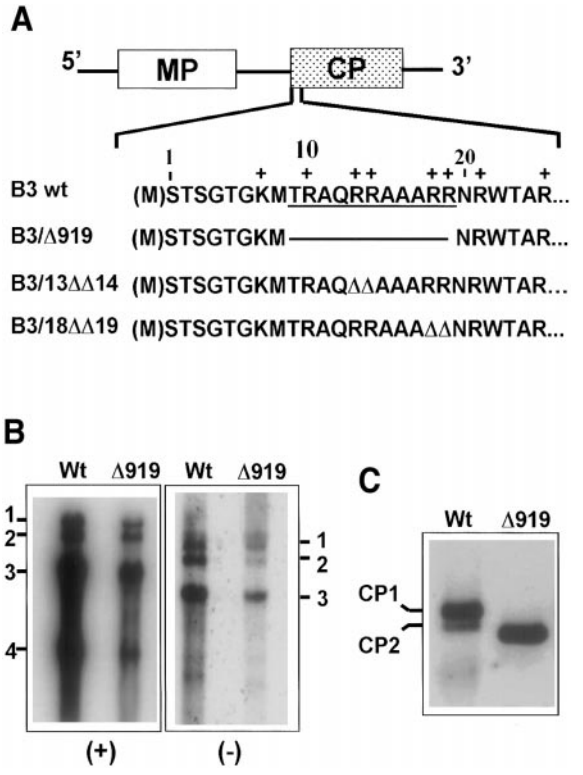

FIG. 1. Characteristics of BMV CP variants used in this study. (A) The structure of wild type (wt) BMV RNA3 (B3) is shown, with noncoding sequences represented as single lines and the movement protein gene (3a) as an open box. The stippled box represents the CP gene. The sequence of the first 25 N-terminal amino acid region, predicted to interact specifically with viral RNA, is shown and the underlined amino acid sequence represents the N-terminal arginine-rich motif (ARM) conserved among plant and nonplant viruses. Positively charged side chains, which are also trypsin cleavage sites, are indicated by (+). In bromoviruses, the initiating methionine (enclosed in parentheses) is removed and the resultant N-terminal serine is acetylated in the mature coat protein (Moosic *et al.,* 1983). In variant B3/Δ919, the deletion of the ARM located between amino acids 8 to 20 is indicated by a solid line. In B3/13ΔΔ14 and B3/18ΔΔ19, deletion of arginine residues located at 13 and14 and 18 and19, respectively, are indicated by Δ. (B) Replication and analysis of progeny (+) and (−) strand RNA of wt B3 and B3/Δ919 in barley protoplasts. Approximately 2.5×10^5 protoplasts were transfected with the desired combination of RNA transcripts and progeny was subjected to Northern blot analysis. The blots were hybridized with ^{32}P-labeled riboprobes of desired specificity and complementary to the conserved 3′ noncoding region. The positions of the three BMV genomic RNAs and a single subgenomic RNA4 are shown. Detection of progeny (+) and (−) strands required 2- and 48-h exposure times, respectively. (C) Western blot analysis of matured CP derived from barley protoplasts transfected with wt B1 and B2, and either wt B3 or B3/Δ919 transcripts. The positions of CP1 (synthesized from the first methionine) or CP2 (synthesized from second methionine located at position 8; panel A) are shown. Note: Deletion of ARM in B3/Δ919 resulted in faster migration of CP.

virion assembly by inoculating *C. quinoa*. Thus, an inoculum containing a mixture of *in vitro* synthesized RNA transcripts of wt B1, B2, and B3/Δ919 was inoculated onto approximately 3-week-old *C. quinoa* plants that had been kept in the dark for at least 18 h. Control inoculations were made with an inoculum containing all three wt

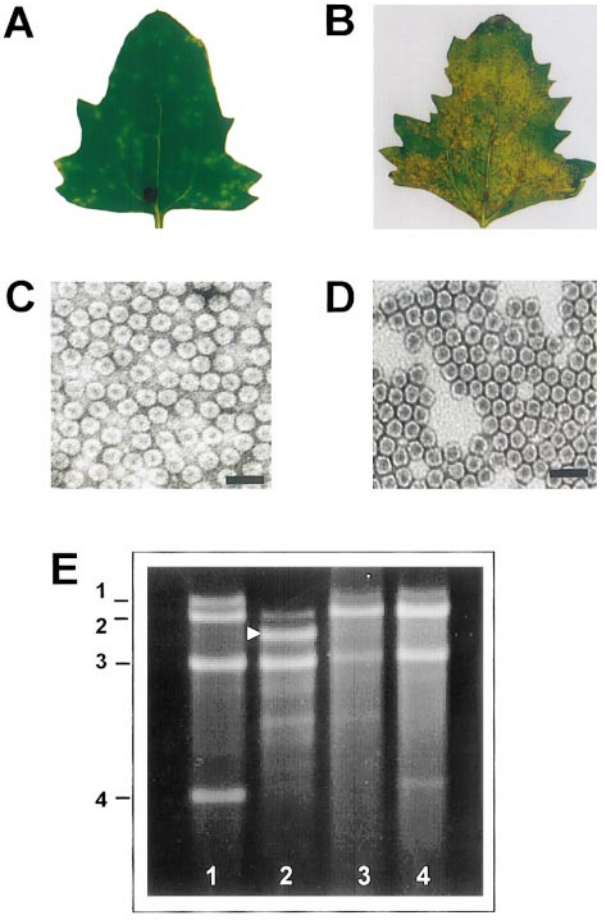

FIG. 2. Symptom phenotypes induced in *Chenopodium quinoa* by an inoculum containing a mixture of wt B1 and B2 and either wt B3 (A) or B3/Δ919 (B) transcripts. The leaves were photographed at 5 days postinoculation (dpi) for wt and 7 dpi for the variant. (C and D) Electron micrographs showing the characteristic features of purified virions of wt (C) and B3/Δ919 (D) recovered from symptomatic leaves of *C. quinoa.* Purified virus preparations were negatively stained with uranyl acetate and photographed at a magnification of 50,000×. Bar = 50 nm. (E) Agarose gel electrophoretic analysis of RNA isolated from purified virions of wt (lane 1), B3/Δ919 (lane 2), B3/13ΔΔ14 (lane 3), and B3/18ΔΔ19 (lane 4). Approximately 1 μg of each virion RNA sample was subjected to electrophoresis in 1% agarose and stained with ethidium bromide. In lane 2, the arrowhead indicates the position of RNA2a component found only in B3/Δ919 virion preparations.

genomic BMV RNA transcripts. As expected, *C. quinoa* plants inoculated with wt control developed chlorotic local lesions (Fig. 2A) 4 to 5 days postinoculation (dpi) and displayed systemic mottling on upper uninoculated leaves 10–12 dpi. By contrast, *C. quinoa* plants inoculated with B3/Δ919 displayed necrotic local lesions which slowly expanded with time resulting in large necrotic blotches (Fig. 2B). None of these plants developed visible systemic symptoms even after 3 weeks postinoculation and no viral RNA could be detected in symptomless uninoculated leaves when a total nucleic acid preparation from these leaves was subjected to Northern blot hybridization and probed with riboprobes specific for BMV RNAs (data not shown).

Truncated CP derived from B3/Δ919 is competent for virion assembly *in vivo*

Since only virion assembly competent variants of B3 can induce local lesions (Rao, 1999), induction of local necrotic lesions following inoculation with B3/Δ919 (Fig. 2B) indicated that a truncated CP from B3/Δ919 could have assembled into virions and potentiated cell-to-cell movement. To substantiate this assumption, virions were purified from symptomatic leaves of *C. quinoa* and examined under an electron microscope. Although virions of B3/Δ919 (Fig. 2D) appeared to be characteristic of BMV in size and morphology, unlike wt BMV virions (Fig. 2C), they had larger electron-dense centers (Fig. 2D), indicating that more uranyl acetate had penetrated into the particles.

Since *Bromoviruses* are stabilized by RNA-protein interactions and the fact that no empty virions accumulate during *Bromovirus* infections *in vivo* (Fox *et al.,* 1995), virions recovered from B3/Δ919-infected *C. quinoa* possibly have packaged BMV RNAs. When RNA extracted from purified virions of wt and B3/Δ919 was analyzed by agarose gel electrophoresis, the profile for B3/Δ919 was distinct from that of wt control (Fig. 2E, lanes 1 and 2). In contrast to the characteristic profile of four BMV RNAs found in the wt control (Fig. 2E, lane 1), only three RNAs were detected for B3/Δ919 (Fig. 2E, lane 2). Two RNAs with electrophoretic mobilities similar to those of BMV genomic RNAs 2 and 3 were evident. An additional RNA component migrating faster than genomic RNA2 (referred to as RNA2a and indicated by an arrowhead in Fig. 2E, lane 2), not found in wt BMV virions, was reproducibly observed in several independent B3/Δ919 virion preparations. No RNA bands characteristic of either BMV genomic RNA1 or subgenomic RNA4 were detected (Fig. 2E, lane 2), suggesting that virions packaging genomic RNA1 and subgenomic RNA4 are less stable or incompletely formed. However, inoculation of *C. quinoa* plants with purified virions of B3/Δ919 resulted in symptom phenotypes similar to those shown in Fig. 2B, indicating particles containing RNA1 are present in the purified preparations. In addition, we also found that storage at −20°C of either symptomatic leaves of *C. quinoa* or purified virions of B3/Δ919 beyond a 2-week period rendered the inocula noninfectious, suggesting that the engineered deletion in BMV CP affected virion stability.

To verify the RNA profile in purified virions, a Northern blot containing total and virion RNA preparations from plants infected with the wt control and B3/Δ919 was hybridized with riboprobes complementary to 3′ noncoding region conserved among all four BMV RNAs (Fig. 3A). As expected, four BMV RNAs are readily detected in total and virion RNA preparations of wt control (Fig. 3A). The

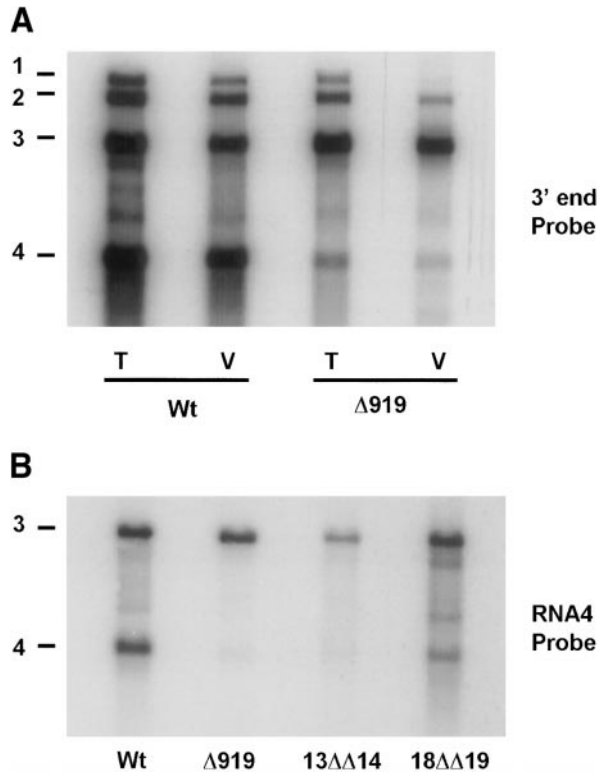

FIG. 3. Progeny RNA analysis of wt BMV and three B3 variants from *C. quinoa* plants. (A) Northern blot analysis of total nucleic acid (T) and virion RNA (V) preparations of wt and B3/Δ919 recovered from symptomatic *C. quinoa* leaves inoculated with wt B1 and B2 and the indicated B3. Approximately 5 μg of total nucleic acid and 200 ng of virion RNA was denatured with glyoxal and subjected to 1% agarose gel electrophoresis prior to electrotransfer to nylon membranes. The blot was hybridized with a ^{32}P-labeled riboprobe complementary to the 3′ noncoding region. The positions of four BMV RNAs are shown to the left. (B) Northern blot analysis of virion RNA of wt and indicated B3 variants obtained from *C. quinoa* leaves. Approximately 200 ng of each virion RNA was denatured and subjected to hybridization with a riboprobe complementary to a portion of the RNA4 sequence (Osman *et al.,* 1998). The positions of BMV genomic RNA3 and subgenomic RNA4 are shown to the left.

total RNA preparations of B3/Δ919 also contained four RNAs, including the subgenomic RNA4 that was not detected by agarose gel electrophoresis (Fig. 2E, lane 2). In these preparations, the levels of subgenomic RNA4 are similar to those observed in protoplasts (i.e., reduced by 90%; Fig. 3A). However, when the levels of virion RNA1 of B3/Δ919 were compared to its level found in total nucleic acid preparations, only trace amounts of full-length genomic RNA1 were detected in virion RNA (Fig. 3A). Likewise, in total RNA preparations genomic RNA2 was synthesized to near wt levels, while 80% of it was found to be packaged (Fig. 3A). Under denaturing conditions RNA2a comigrated with genomic RNA3 (see Fig. 4G, lane 3) and therefore the packaging efficiency of B3/Δ919 RNA3 could not be quantitated using the Northern blots shown in Fig. 3A. Thus, another Northern blot containing virion RNAs was hybridized with a riboprobe complementary to RNA4 sequence (Fig. 3B). Quantitative analysis of this blot revealed that RNA3 derived from B3/Δ919 was packaged with the same efficiency as that of wt control (Fig. 3B). Interestingly, RNA2a found in the virions of B3/Δ919 (Fig. 2E, lane 2) was not detected by the 3′-end probe and subsequent experiments revealed that it comigrated with genomic RNA3 (see Fig. 4G, lane 3). The levels of encapsidated subgenomic RNA4 were found be severely debilitated as compared with that of wt control when the blots were hybridized with a riboprobe specific for CP gene sequence (Fig. 3B).

Molecular characterization of RNA2a

To determine the origin and sequence of RNA2a species found in the virions of B3/Δ919 (Fig. 2E, lane 2), this RNA fragment was purified from virion RNA preparation using low-melting-point agarose gel electrophoresis. Initial Northern hybridization analysis using riboprobes specific for each of the three genomic RNAs revealed that the RNA2a fragment originated from genomic RNA1, since it did not hybridize to riboprobes specific for RNA2 or RNA3 (data not shown). Thus, to further characterize the sequence of RNA2a, a series of Northern blots each containing RNA2a along with virion RNA of wt BMV and B3/Δ919 as controls, were produced and hybridized with five independently synthesized riboprobes encompassing the entire BMV genomic RNA1 (excluding the highly conserved 3′ noncoding region). Results of these hybridization experiments are shown in Fig. 4.

Hybridization of total RNA recovered from leaves inoculated with wt BMV and B3/Δ919 with a riboprobe specific for RNA1 detected full-length genomic RNA1 (Fig. 4A). However, hybridization of virion RNA of B3/Δ919 with riboprobes specific for RNA1 revealed a distinct profile. For example, in control lanes containing wt BMV RNA, only one RNA species was hybridized to each of the five riboprobes (lanes 1 in Figs. 4B–4F). By contrast, hybridization of virion RNA preparations of B3/Δ919 with the same set of riboprobes detected a weaker signal for genomic RNA1 and several faster migrating RNA species of varying size, the smallest of which was approximately 600 nucleotides [nt; indicated with an asterisk (*) in Fig. 4A, lane 2]. Since none of these faster migrating RNAs was detected with a riboprobe complementary to the 3′ highly conserved noncoding region (Fig. 4G, lane 2), they all lacked at least the 3′ 200 terminal nt.

When gel purified RNA2a was analyzed under denaturing conditions, its mobility was approximately correlated with that of BMV RNA3 (Fig. 4G; lane 3). This suggested that a deletion of approximately 1100 nt from genomic RNA1 had occurred to yield RNA2a. Since a riboprobe complementary to the 3′ tRNA-like sequence strongly hybridized to RNA2a (Fig. 4G, lane 3), the deletion must have occurred upstream of the 3′-end sequence. Therefore to identify the missing sequences in

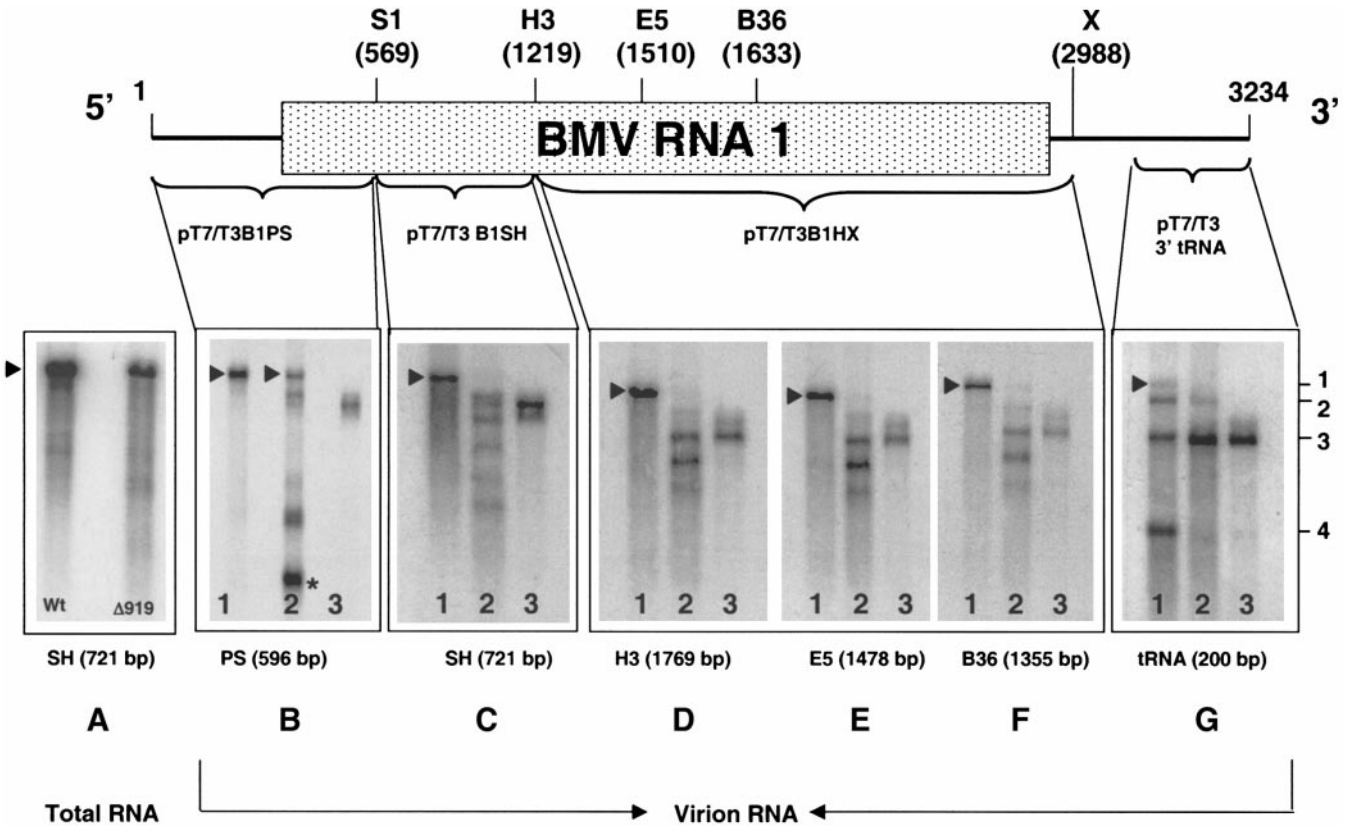

FIG. 4. Characterization of virion RNA of B3/Δ919 and RNA2a. Schematic representation of the structure of BMV genomic RNA1. The noncoding sequences are represented as solid lines. The coding region is shown as a stippled box. The position of selected restriction sites used for subcloning desired sequences, for riboprobe synthesis, is also shown. Selected sequences cloned into pT7/T3–18U vector are indicated by brackets. For example, plasmid pT7/T3B1SH was constructed by subcloning BMV RNA1 sequence present between *Sac*I (located at position 569) and *Hin*dIII (located at position 1219). S1, *Sac*I; H3, *Hin*dIII; E5, *Eco*RV; B36, *Bsu*36I; X, *Xba*I. (A) An autoradiograph of Northern blot containing total RNA preparations recovered from *C. quinoa* inoculated with either wt or B3/Δ919. The blot was hybridized with BMV RNA1-specific riboprobe synthesized from pT7/T3B1SH. The arrowhead indicates the position of BMV RNA1. (B–G) Autoradiographic images of Northern blots containing (1) virion RNA of wt BMV, (2) virion RNA of B3/Δ919, and (3) gel purified RNA2a. Blots B and C, respectively, were hybridized with a riboprobe derived from pT7/T3B1PS and pT7/T3B1SH. Blots D–F were hybridized with riboprobes derived from pT7/T3B1HX by linearizing with either *Hin*dIII (D), *Eco*RV (E), or *Bsu*36I (F). Blot shown in (G) was hybridized with a riboprobe complementary to 3′ tRNA-like structure common to all four BMV RNAs. The size of the riboprobe used to hybridize each blot is shown. The positions of three BMV genomic RNAs and a single subgenomic RNA4 are shown on right. The arrowhead in each panel represents the position of full-length genomic RNA. An asterisk (*) in blot (B) represent the 600-bp fragment derived from genomic RNA1.

RNA2a, multiple Northern blots containing purified RNA2a were hybridized with five independent riboprobes encompassing different regions of RNA1 (Figs. 4B–4F). We are unable to precisely determine the extent of deletion in RNA2a, since all five probes hybridized to RNA2a with varying intensities.

Our attempts to amplify and clone the purified RNA2a using primers complementary to 5′ and 3′ terminal sequences of wt RNA1 in an RT-PCR reaction were unsuccessful, although a cDNA fragment of the expected size was amplified in control samples containing transcripts of wt BMV RNA1. On the basis of Northern hybridization results presented in Fig. 4, a series of 5′-terminal primers in combination with a common 3′-terminal primer were used in RT-PCR. A positive PCR fragment was obtained for RNA2a only when a 5′ primer complementary to a sequence between 953 and 979 nt (^{953}ACGCTGCCCCGGGAGACACTACGTCA^{979}), but not with a sequence upstream to position 953, was present in the reaction. This suggested that RNA2a had lost a sequence upstream of 953 nt. By using primer extension we identified that RNA2a had lost the 5′ 943 nt. These observations indicate that at least one of the major binding sites for the N-terminal ARM resides within the first 5′ 900 nt of BMV RNA1. This assumption is further supported by the findings of Duggal and Hall (1993) that one of the two CP binding sites on BMV RNA1 is located between 668 and 1290 nt. Taken together, it seems that the interaction between the N-terminal ARM of BMV CP and the 5′ 943 nt of BMV genomic RNA1 is crucial for the stability of packaged RNA1. Absence of specific interaction perhaps destabilized the particles and exposed the RNA1 to nuclease attack, resulting in the fragmentation observed (Figs. 4B–4F, lanes 2).

Arginine residues at positions 13 and 14 are specific for packaging BMV subgenomic RNA4

The first 25 N-terminal amino acids of a BMV CP contain eight positively charged residues (one lysine and seven arginines; Fig. 1A). The biological activity of B3/Δ919 and encapsidation competence of its truncated CP revealed that five arginine residues contained within the deleted region (i.e., at positions 10, 13, 14, 18, and 19; Fig. 1A) either independently or collectively are likely to contribute to the specific binding and/or packaging of BMV RNAs. To identify which of the four arginine residues are critically involved in RNA interactions, two additional deletion variants of B3 were constructed (Fig. 1B). In variants B3/13ΔΔ14 and B3/18ΔΔ19 (Fig. 1B), two consecutive arginine residues located at either position 13 and 14 or 18 and 19, respectively, are deleted. Independent inoculation of these two variant B3 transcripts (in combination with wt B1 and B2) were infectious to *C. quinoa*. Interestingly, only B3/18ΔΔ19, but not B3/13ΔΔ14, was competent to move systemically in this host. Agarose gel electrophoretic analysis of RNA isolated from purified virions of B3/13ΔΔ14 and B3/18ΔΔ19 revealed a profile distinct from that of B3/Δ919 (Fig. 2E, compare lane 2 with lanes 3 and 4). Unlike B3/Δ919, CP synthesized from B3/13ΔΔ14 and B3/18ΔΔ19 packaged near wt levels of genomic RNA1, whereas B3/13ΔΔ14, but not B3/18ΔΔ19, failed to package subgenomic RNA4 to detectable levels (Fig. 2E, lanes 3 and 4) and only a trace amount was detected by Northern blot analysis (Fig. 3B). Interestingly, a reduction of 30% in RNA3 packaging was observed for B3/13ΔΔ14 (Fig. 2E, lane 3; Fig. 3B) but not for B3/18ΔΔ19 (Fig. 2E, lane 4; Fig. 3B). Virions of these two variants contained near wt levels of full-length genomic RNA1 and, unlike B3/Δ919, no fragmented RNA1 similar to RNA2a was detected (Fig. 2E).

In vitro reassembly assays demonstrate that CPs derived from B3/Δ919 and B3/13ΔΔ14, but not B3/18ΔΔ19, are specifically defective in packaging subgenomic RNA4

Like that of BMV RNA1, hybridization of virion RNA of B3/Δ919 with a riboprobe specific for RNA4 did not reveal any indication of RNA4 fragmentation (Fig. 3B). Therefore, it is likely that low levels of RNA4 seen in total and virion RNA of B3/Δ919 (Figs. 3A and 3B) could be the result of defective packaging of RNA4 by the truncated CPs. To verify this possibility a series of *in vitro* reassembly experiments between BMV CP and RNA were performed. Purified *Bromovirus* preparations can be dissociated into protein and RNA and can be reassembled *in vitro* to yield virions like those found in natural infections (Fox *et al.,* 1994). A variety of conditions that facilitate the reassembly of bromovirus RNA and protein have been described (Fox *et al.,* 1994; Zhao *et al.,* 1995). Although no empty virions have been found *in vivo* (Fox *et al.,* 1994), either empty or RNA-containing virions or both can be assembled *in vitro* using different assay conditions. Thus, when CP and RNA are allowed to reassemble in buffer A (1 M NaCl, 50 mM NaAc, pH 4.8, 10 mM KCl, 5 mM $MgCl_2$, and 1 mM DTT) both empty and RNA-containing virions are formed. By contrast, reassembly in buffer B (50 mM NaCl, 50 mM Tris, pH 7.2,10 mM KCl, 5 mM $MgCl_2$, and 1 mM DTT) results in the formation of RNA-containing virions only. Since the major objective of this study is to examine the competence of mutant CPs to package BMV RNAs under conditions which closely reflect those seen the plant cell, all reassembly assays were done using buffer B. To synthesize full-length RNA4 transcripts, a plasimd pT7B4 (Fig. 5) containing a cDNA copy of RNA4 was constructed. *In vitro* transcription of this plasmid resulted in the synthesis of RNA4 transcripts identical to those found in wt BMV virions.

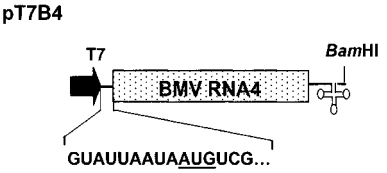

FIG. 5. Schematic representation of pT7B4. The entire sequence of subgenomic RNA4, identical to that found in wt BMV, is positioned under the control of a T7 promoter (indicated by arrow at the 5′ end) with the start of transcription corresponding to the 5′ end of RNA4. Single lines represent noncoding regions and stippled box represents coat protein ORF. The sequence of a 9-base leader and the CP start codon (underlined) is shown. The DNA template was linearized with *Bam*HI (shown at the 3′ end) prior to *in vitro* transcription.

Two sets of *in vitro* reassembly assays were performed to test the competence of CP of B3/Δ919 to package BMV subgenomic RNA4. Reassembly using CP from wt BMV served as a control. In the first set of experiments, all four wt BMV RNAs recovered from purified virions were supplied as substrates for CPs of either wt BMV or B3/Δ919. In the second set, *in vitro* synthesized transcripts of either full-length genomic RNA1 or RNA4 were used. In addition, we also examined whether CP of B3/Δ919 is competent for assembly into virions when purified RNA2a is supplied as a substrate. Results of these *in vitro* reassembly assays are summarized in Fig. 6 and Table 1.

We observed that the reassembly process between BMV CP and a given RNA is highly specific under the conditions tested, since icosahedral virions were assembled only when homologous BMV genomic RNAs were provided as substrates, but not heterologous *Xenopus* RNA (1.5 kb; Table 1). As expected, absence of any RNA in the reaction did not result in empty capsid formation (Table 1). In the first set of reassembly assays, as evidenced from Northern blot hybridization, wt CP packaged all four BMV RNAs (Fig. 7A, lane 1), whereas CP of B3/Δ919 packaged only three of the four BMV RNAs (Fig. 7A; lane 2). Reassembly assays between wt CP and

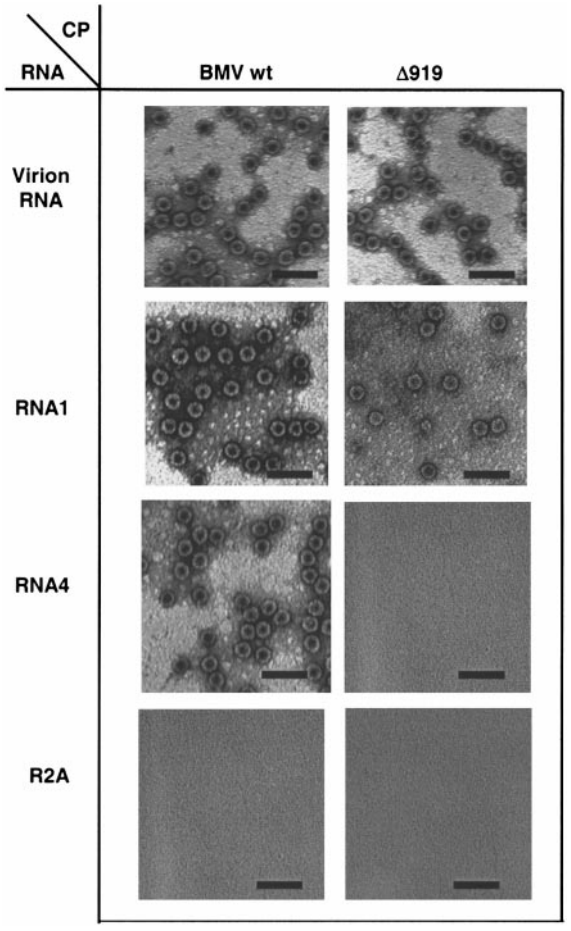

FIG. 6. *In vitro* reassembly assays. Electron micrographic images showing the negatively stained preparations of *in vitro* reassembled particles from purified CP of either wt BMV or B3/Δ919 and the indicated RNAs. Bar = 100 nm.

either genomic RNA1 or subgenomic RNA4 also resulted in formation of virions identical to those observed in natural infections (Fig. 6; Fig. 7B; lanes 1 and 4; Table 1). Likewise, the CP of B3/Δ919 also efficiently packaged full-length genomic RNA 1 (Fig.7B) and did not result in fragmentation that was seen in virions recovered from symptomatic leaves. These observations indicate that CP of B3/Δ919 is not defective in packaging RNA1, while fragmentation of RNA1 (Figs. 4B–4F) could have been the result of specific instability of RNA1-containing virions during the purification procedure.

By contrast to genomic RNA1, transcripts of subgenomic RNA4 were not packaged by the CP of B3/Δ919 (Fig. 7B, lanes 5 and 7; Table 1), confirming that CP of B3/Δ919 is specifically defective in packaging BMV subgenomic RNA4. Purified RNA2a was not assembled into virions with the CP of either wt or B3/Δ919 (Fig. 7B, lanes 3 and 6; Table 1), indicating that sequences deleted in RNA2a are important for interaction with CP during virion assembly. Similar *in vitro* reassembly assays were performed with CPs of B3/13ΔΔ14 and B3/18ΔΔ19 (Table 1). As observed *in vivo*, CP of B3/13ΔΔ14, but not that of B3/18ΔΔ19, is exclusively defective in packaging subgenomic RNA4 (Table 1).

Previously it was demonstrated that deletion of the first 7 N-terminal amino acids containing a single lysine residue from the matured BMV CP did not reveal any packaging defects (Rao and Grantham, 1995, 1996; Sacher and Ahlquist, 1989). In this study, the *in vivo* packaging competence of arginine-rich motif-defective CPs translated from the subgenomic RNAs of B3/Δ919 and B3/13ΔΔ14 revealed previously unrecognized features of the interactions between BMV RNA and the CP N-terminal basic arm. The N-terminal ARM located between amino acid positions 8 and 20 of BMV CP primarily contains regions essential for specific and discrete interactions with BMV genomic RNA1 and subgenomic RNA4 (Figs. 3 and 4). For example, although wt level full-length genomic RNA1 was consistently recovered from symptomatic leaves of B3/Δ919 (Fig. 4A), virions purified from the same tissue contained only trace amounts of full-length genomic RNA1 and a series of 5′ coterminal truncated RNA1 fragments (Figs. 4B–4F), suggesting that deletion of the entire ARM region of BMV CP, but not parts of it as exemplified by B3/13ΔΔ14 and B3/18ΔΔ19 (Fig. 2E), affected the stability of particles containing RNA1. By contrast the stability of particles containing BMV genomic RNAs 2 and 3 appear to be independent of the N-terminal ARM, since CP variants examined in this study did not exert the same effect that was seen for virions containing RNA1 (Figs. 2 and 3). In

TABLE 1

In Vitro Reassembly Assays[a]

RNAs	Coat Protein[b]			
	Wt BMV	B3Δ919	B3/13ΔΔ14	B3/18ΔΔ19
I. Virion RNA	+[c]	+[d]	+[d]	+[c]
II. Transcripts				
(A) RNA1	+	+	+	+
(B) RNA4	+	−	−	+
III. RNA2a[e]	−	−	NT	NT
IV. *Xenopus* RNA[f]	−	−	−	−
V. No RNA	−	−	−	−

[a] *In vitro* reassembly assays were performed according to Zhao *et al.* (1995) and examined under EM. (+) indicates presence of virions; (−) indicates absence of virions; NT, not tested.

[b] $CaCl_2$ method was used to isolated coat protein from density gradient purified virus preparations.

[c] All four BMV RNAs were found to be packaged by Northern blot analysis.

[d] Only the three genomic RNAs were found to be packaged by Northern blot analysis.

[e] RNA2a was purified on low-melting-point agarose from virions of B3/Δ919.

[f] *In vitro* transcripts of *Xenopus* RNA (1.5 kb) were obtained from a clone provided in the MEGAscript kit (Ambion).

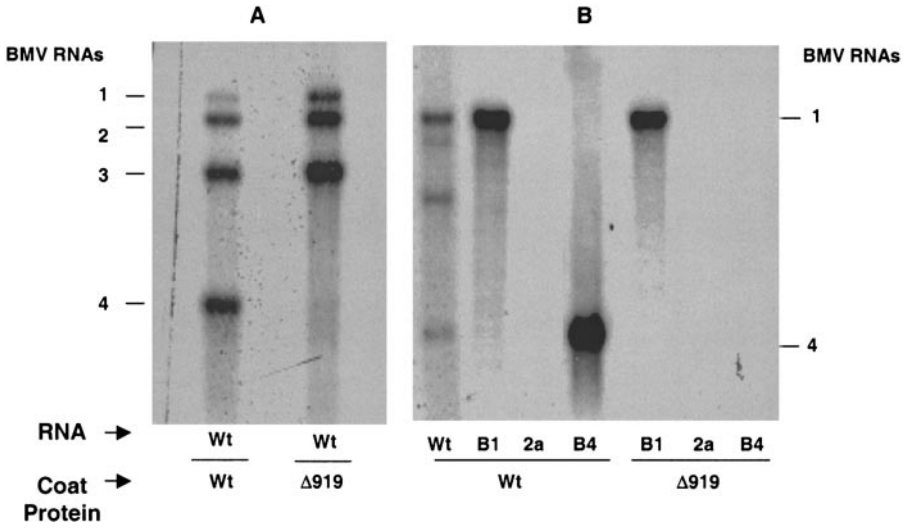

FIG. 7. Northern blot analysis of RNA isolated from *in vitro* reassembled virions. Conditions for denaturation of RNA, electrophoresis, and hybridization with riboprobes are as described under Fig. 3. Blot A was hybridized with a riboprobe complementary to 3′ tRNA-like region, whereas blot B was hybridized with a mixture of riboprobes complementary to 3′ tRNA-like region and specific for BMV genomic RNA1 derived from pT7/T3B1SH (Fig. 4). The position of four BMV RNAs is shown to the left and the positions of BMV RNAs 1 and 4 are shown to the right.

view of these findings, we speculate that signals for recognizing genomic RNA1 and subgenomic RNA4 are localized within the N-terminal ARM of BMV CP, while those required for genomic RNAs 2 and 3 resided elsewhere in the CP.

A most significant outcome of this study is the defective packaging trait exhibited by the CPs of B3/Δ919 and B3/13ΔΔ14 *in vivo* and *in vitro* for subgenomic RNA4. Although BMV RNA3 and 4 are predicted to be copackaged into one particle, our data indicate genomic RNA3 can be packaged independent of subgenomic RNA4, since virions purified from symptomatic leaves of B3/Δ919 and B3/13ΔΔ14 contained only RNA3 but not RNA4 (Figs. 6 and 7B). This conjecture is supported by the recent demonstration of independent packaging of BMV CP mRNA into virions assembled from 120 CP subunits in yeast cells (Krol *et al.,* 1999). The specific packaging defect of subgenomic RNA4 exhibited by B3/13ΔΔ14 suggests that positively charged arginine residues located at positions 13 and 14 are intimately involved in packaging. Alternatively, structural features of the region containing the deletion could also exert constraints that lead to defective packaging. For example, previous NMR studies with cowpea chlorotic mottle bromovirus (CCMV) CP showed that the N-terminal basic arm assumes an α-helical conformation upon binding of RNA or oligophosphates to the region between residues 8 and 18 (Vriend *et al.,* 1986; Van der Graaf *et al.,* 1992). Thus, it is likely that the N-terminal α-helical conformation might play an important role in RNA binding and subsequent virion assembly in *Bromoviruses*. Since amino acid residues outside the ARM are also required for wt activity (Burd and Dreyfuss, 1994), a full understanding of the structure and RNA-binding properties of ARM domains will require examination of the rest of the protein.

MATERIALS AND METHODS

In vitro transcription, protoplast assays, whole plant inoculations, and Western blot analysis

Throughout these studies biologically active clones corresponding to BMV RNA1 (B1), RNA2 (B2), and RNA3 (B3) were used (Dreher *et al.,* 1989; Rao *et al.,* 1989). Deletions were engineered into a biologically active clone of B3 using PCR (Rao and Grantham, 1995, 1996). Synthesis of capped *in vitro* RNA transcripts from wt and variant clones, replication assays in protoplasts, and detection and quantification of progeny RNA are as described previously (Rao *et al.,* 1989, 1994). The biological activity of wt and variant clones was tested on *Chenopodium quinoa* (Rao and Grantham, 1995). Encapsidation assays were done by micropurification as described previously (Rao and Grantham, 1995). For Western blot analysis, CP samples were fractionated on a 16% SDS–PAGE and transferred to nitrocellulose membrane. CP was detected using anti-BMV CP and a chemiluminescent kit (Osman *et al.,* 1998).

Northern blot analysis and plasmids for riboprobes

For Northern blot analysis, nucleic acid preparations were denatured with glyoxal, electrophoresed in 1% agarose gels, and electrophoretically transferred to Nytran membranes (Rao *et al.,* 1994). Each blot was hybridized with ^{32}P-labeled riboprobes of desired strand and RNA species specificity. To synthesize riboprobes encompassing a specific region within the BMV RNA1 sequence, three individual clones were constructed (Fig. 4): (1) Plasmid pT7T3/B1PS was constructed by cloning a *Pst*I-*Sac*I fragment encompassing 5′ 596 bases from

pT7B1 into pT7/T3–18U; (2) Plasmid pT7T3/B1SH was constructed by cloning 721 bases from pT7B1 as *Sac*I-*Hin*dIII fragment into pT7/T3–18U; and (3) Plasmid pT7/T3HX was constructed by cloning 1769 bases from pT7B1 as *Hin*dIII-*Xba*I fragment into pT7/T3–18U. A T7 transcript from all these vectors was used to detect progeny (+) RNA. Primer extension was done according to Sambrook *et al.* (1989).

Coat protein preparation, *in vitro* reassembly assays, and electron microscopy

Purified BMV virions of either wt or variants were dissociated into coat protein by dialyzing at 4°C for 24 h against a buffer containing 500 mM $CaCl_2$, 50 mM Tris–HCl, pH 7.5, 1 mM EDTA, 1 mM DTT, and 0.5 mM PMSF (Verduin, 1978). Following a low-speed centrifugation at 14,000 *g* for 30 min, the supernatant was subjected to 155,000 *g* for 2 h to remove intact virions. Dissociated coat protein concentration was determined by a spectrophotometer. *In vitro* reassembly assays were done essentially as described by Zhao *et al.* (1995). Briefly, CP and desired RNA transcripts were mixed in ratio of 1:5 (wt/wt) and dialyzed at 4°C for 24 h against an assembly buffer containing 50 mM NaCl, 50 mM Tris–HCl, pH 7.2, 10 mM KCl, 5 mM $MgCl_2$, and 1 mM DTT. The assembled virions were concentrated by using Centricon-100 microconcentrators (Amicon, Beverley, MA), and suspended in virus stabilization buffer (sodium citrate buffer, pH 4.8). *In vitro* reassembled virions were negatively stained with 1% uranyl acetate and examined under a Hitachi transmission electron microscope. RNA was isolated from nuclease resistant *in vitro* reassembled virions and analyzed by Northern blots.

ACKNOWLEDGMENTS

We thank Mark Young for providing a protocol for *in vitro* reassembly assays, and Chen Kao and Anthony Clark for helpful discussions. Research in this laboratory was supported by a grant from the USDA NRICGP (9935303).

REFERENCES

Ahlquist, P. (1994). Bromoviruses. *In* " Encyclopedia of Virology" (R.G. Webster and A. Granoff, Eds.), Vol. 1, pp 181–185. Academic Press, San Diego, CA.

Burd, C. G., and Dreyfuss, G. (1994). Conserved structures and diversity of functions of RNA-binding proteins. *Science* **265,** 615–621.

Dreher, T. W., Rao, A. L. N., and Hall, T. C. (1989). Replication *in vivo* of mutant brome mosaic virus RNAs defective in aminoacylation. *J. Mol. Biol.* **206,** 425–438.

Duggal, R., and Hall, T. C. (1993). Identification of domains in brome mosaic virus RNA-1 and coat protein necessary for specific interaction and encapsidation. *J. Virol.* **67,** 6406–6412.

Fox, J. M., Johnson, J. E., and Young, M. (1994). RNA/protein interactions in icosahedral virus assembly. *Semin. Virol.* **5**, 51–60.

Krol, M. A., Olson, N. H., Tate, J., Johnson, J. E., Baker, T. S., Ahlquist, P. (1999). RNA-controlled polymorphism in the *in vivo* assembly of 180-subunit and 120-subunit virions from a single coat protein. *Proc. Natl. Acad. Sci. USA* **96,** 13650–13655.

Lazinski, D., Grzatzielska, E., and Das, A. (1989). Sequence-specific recognition of RNA hairpins by bacteriophage antiterminators requires a conserved arginine-rich motif. *Cell* **59,** 207–218.

Miller, W. A., Dreher, T. W., and Hall, T. C. (1985). Synthesis of brome mosaic virus subgenomic RNA in vitro by initiation on (−) sense genomic RNA. *Nature* **313,** 68–70.

Moosic, J. P., McKean, D. J., Sish, D. S., and Kaesberg, P. (1983). Primary structure of brome mosaic virus coat protein. *Virology* **129,** 517–520.

Osman, F., Choi, Y. G., Grantham, G. L., and Rao, A. L. N. (1998). Molecular studies on bromovirus capsid protein. V. Evidence for the specificity of brome mosaic virus encapsidation using RNA3 chimera of brome mosaic and cucumber mosaic viruses expressing heterologous coat proteins. *Virology* **251,** 438–448.

Rao, A. L. N. (1999). Molecular basis of symptomatology. *In* "Molecular Biology of Plant Viruses" (C. L. Mundahar, Ed.), pp. 201–210. Kluwer Academic, Boston, MA.

Rao, A. L. N., Dreher, T. W., Marsh, L. E., and Hall, T. C. (1989). Telomeric function of the tRNA-like structure of brome mosaic virus RNA. *Proc. Natl. Acad. Sci. USA* **86,** 5335–5339.

Rao, A. L. N., Duggal, R., Lahser, F., and Hall, T. C. (1994). Analysis of RNA replication in plant viruses. *In* "Methods in Molecular Genetics: Molecular Virology Techniques" (K. W. Adolph, Ed.), Vol. 4, pp. 216–236. Academic Press, Orlando, FL.

Rao, A. L. N., and Grantham G. L. (1995). Biological significance of the seven amino-terminal basic residues of brome mosaic virus coat protein. *Virology* **211,** 42–52.

Rao, A. L. N., and Grantham, G. L. (1996). Molecular studies on bromovirus capsid protein. II. Functional analysis of the amino terminal arginine rich motif and its role in encapsidation, movement and pathology. *Virology* **226,** 294–305.

Sacher, R., and Ahlquist, P. (1989). Effects of deletions in the N-terminal basic arm of brome mosaic virus coat protein on RNA packaging and systemic infection. *J. Virol.* **63,** 4545–4552.

Sambrook, J., Fritsch, E. F., and Maniatis, T. (1989). " Molecular cloning: A Laboratory Manual," 2nd ed. Cold Spring Harbor Laboratory Press, Cold Spring Harbor, NY.

Schmitz, I., and Rao, A. L. N. (1996). Molecular studies on bromovirus capsid protein: I. Characterization of cell-to-cell defective RNA3 variants of brome mosaic virus. *Virology* **226,** 281–293.

Sgro, J., Jacrot, B., and Chroboczek, J. (1986). Identification of regions of brome mosaic virus coat protein chemically cross-linked *in situ* to viral RNA. *Eur. J. Biochem.* **154,** 69–76.

Speir, J. A., Munshi. S., Wang, S., Baker, T. J., and Johnson, J. E. (1995). Structures of the native and swollen forms of cowpea chlorotic mottle virus determined by X-ray crystallography and cryoelectron microscopy. *Structure* **3,** 63–78.

Tan, R., and Frankel, A. D. (1995). Structural variety of arginine-rich RNA binding peptides. *Proc. Natl. Acad. Sci. USA*, **92,** 5282–5286.

Van der Graaf, M., Scheek, R. M., van der Linden, C. C., and Hemminga, M. A. (1992). Conformation of a pentacosapeptide representing the RNA-binding N-terminus of cowpea chlorotic mottle virus coat protein in the presence of oligophosphates: A two-dimensional proton nuclear magnetic resonance and distance geometry study. *Biochemistry* **31,** 9177–9182.

Verduin, B. J. M. (1978). Degradation of cowpea chlorotic mottle virus ribonucleic acid *in situ. J. Gen. Virol.* **39,** 131–147.

Vriend, G., Verduin, B. J. M., and Hemminga, M. A. (1986). Role of the N-terminal part of the coat protein in the assembly of cowpea chlorotic mottle virus: A 500 MHz proton nuclear magnetic resonance study and structural calculations. *J. Mol. Biol.* **191,** 453–460.

Zhao, X., Fox, J. M., Olson, N. H., Baker, T. M., and Young, M. J. (1995). *In vitro* assembly of cowpea chlorotic mottle virus from coat protein expressed in *Escherichia coli* and *in vitro*-transcribed viral cDNAs. *Virology* **207,** 486–494.